Carbohydrate Polymers 82 (2010) 802–808

Contents lists available at ScienceDirect

Carbohydrate Polymers

journal homepage: www.elsevier.com/locate/carbpol

Poly (butylensuccinate co-adipate)-thermoplastic starch nanocomposite blends

S. Bocchini*, D. Battegazzore, A. Frache

Politecnico di Torino, Dipartimento di Scienze dei Materiali e Ingegneria Chimica, V.le Teresa Michel 5, Alessandria 15121, Italy

ARTICLE INFO

Article history:
Received 11 April 2010
Received in revised form 25 May 2010
Accepted 26 May 2010
Available online 4 June 2010

Keywords:
Biopolymers
Nanocomposite
Thermoplastic starch

ABSTRACT

Nanocomposites based on blends of thermoplastic corn starch (TPS), plasticized with glycerol, and poly (butylensuccinate co-adipate) (PBAS) were prepared using sodium montmorillonite and organomodified montmorillonite. X-ray diffraction and scanning electron microscopy were used to study the clay dispersion. The effects of PBAS and clay type content on mechanical properties were evaluated. TPS/PBAS/organic modified montmorillonite shows an exfoliated nanocomposite structure and a notable increase of the modulus.

1. Introduction

The depletion in fossil feedstocks, increasing oil prices and the ecological problems associated with CO_2 emissions are forcing the development of alternative resources for chemicals. On the other hand environmentally friendly processes are highly regarded due to growing concerns about pollution. The use of biodegradable plastics obtained from natural resources is seen as a strategy to minimise the environmental impact and develop sustainable plastics. There are many biodegradable plastics and/or from natural source (Belgacem & Gandini, 2008). Synthetic biodegradable polymers, although having excellent properties, are costly and typically manufactured using non-renewable petroleum resources. Natural polymers such as starch-based thermoplastics, which are manufactured using an annually renewable source as raw material, are relatively cheap.

Native starch can be transformed into a thermoplastic material, thermoplastic starch (TPS), through thermo-mechanical treatment in the presence of suitable plasticizers, such as water and glycerol (Wiedmann & Strobel, 1991). TPS is thus derived from renewable sources, totally compostable and a rather cheap material compared to synthetic thermoplastics. Furthermore TPS can be easily processed with plastic processing machines, it shows a wide properties range according to the plasticizer level and the starch botanical source. On the other hand TPS shows a number of shortcomings such as moisture sensitivity and lower mechanical properties for some applications (e.g. packaging) (Bhattacharya, 1998; Shogren, 1997).

To overcome these shortcomings various efforts were made. Chemical modification of starch has been elaborated on the basis of previews work on cellulose (Fringant, Desbrieres, & Rinaudo, 1996; Mullen & Pacsu, 1942, 1943). This strategy strongly depends on the cost of processing/product purification and by-products toxicity which limits the substitution of traditional plastic materials.

Recent researches (Chivrac, Gueguen, et al., 2008; Chivrac, Pollet, & Avérous, 2009; Chivrac, Pollet, Schmutz, & Avérou, 2008; Chivrac, Pollet, Schmutz, & Avérous, 2010; Cyras, Manfredi, Ton-That, & Vázquez, 2008; Dean, Yu, & Wu, 2007; Ma, Yu, & Wang, 2007; Pandey & Singh, 2005; Park, Lee, Park, Cho, & Ha, 2003; Park et al., 2002) have proved potential of organoclays for starch-based polymer nanocomposites to improve the long-term mechanical properties over the unfilled formulations.

Another more promising strategy has been developed based on blending of TPS with biodegradable polyesters (Avérous, 2004) such as polycaprolactone (PCL) (Amass, Amass, & Tighe, 1999; Avérous, Moro, Dole, & Fringant, 2000; Bastioli, Cerruti, Guanella, Romano, & Tosin, 1995; Koenig & Huang, 1995; Matzinos, Tserki, Kontoyiannis, & Pan, 2001; Myllymäki et al., 1998; Vikman, Hulleman, Van Der Zee, Myllärinen, & Feil, 1999), poly (butylene adipate co-succinate) PBAS (Avérous & Fringant, 2001), poly (butylene adipate-co-terephthalate) (PBAT) (Avérous & Fringant, 2001), polylactic acid (PLA) (Martin & Avérous, 2001), or poly (hydroxy ester ether) (PHEE) (Bastioli, 1998). These commercially available polyesters show more hydrophobic character, a lower water permeability and improved mechanical properties, compared to TPS.

The aim of this research is to prepare a montmorillonite-based nanocomposite blend of thermoplastic starch with an aliphatic polyester in order to improve mechanical properties while

* Corresponding author at: Politecnico di Torino, Dipartimento di Scienze dei Materiali e Ingegneria Chimica, Viale T. Mchel 5, Alessandria 15121, Italy.
Tel.: +39 0131229305; fax: +39 0131229399.
E-mail address: sergio.bocchini@polito.it (S. Bocchini).

0144-8617/$ – see front matter © 2010 Elsevier Ltd. All rights reserved.
doi:10.1016/j.carbpol.2010.05.056

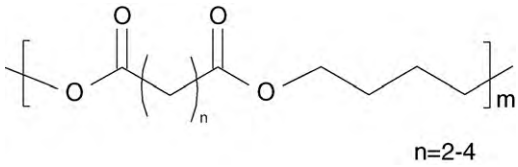

Fig. 1. Poly (butylene adipate co-succinate) (PBAS).

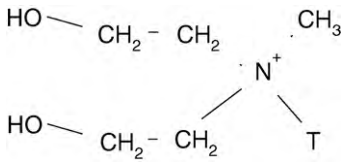

Fig. 2. Methyl, hydrogenated tallow, bis-2-hydroxyethyl, quaternary ammonium.

maintaining biodegradability. The cost of the biodegradable plastic is a limiting factor to develop commercially viable product. Therefore, to develop some economically viable biodegradable materials, starch (excluding thus plasticizer such as glycerol) should remain the major phase in the blend thus polyester content was limited to 20% in weight. PBAS was chosen for the glass transition below room temperature, the higher modulus respect to other polyesters (e.g. PBAT) and a melting temperature not too far from TPS processing temperature.

2. Experimental

2.1. Materials

The starch used was the maize starch CERESTAR RG 03408 (Cargill). The composition of starch is: about 26% amylose, 74% amylopectin, with minor amounts of lipids, proteins and phosphorus compounds. Glycerol with purity ≥99.0% (Aldrich) was used as plasticizer.

The poly (butylene adipate co-succinate) (PBAS) used in blends with TPS was PBI 001 from Natureplast (Fig. 1). Mechanical properties are summarized in Table 1.

The fillers used are a natural montmorillonite modified with methyl, hydrogenated tallow, bis-2-hydroxyethyl, quaternary ammonium (Fig. 2) Cloisite 30B (Cl30B) and a sodium montmorillonite Cloisite Na (ClNa) supplied by Southern Clay Products Inc.

The materials were dried in a oven at 80 °C below 25 mbar pressure for 5 h before blending, the moisture content was kept below 0.1 wt% as tested by Karl–Fischer titration.

The compounds were melt-blended using an internal mixer PLE 67152 (Brabender), residence time 10 min, screw speed 100 rpm, temperature 120 °C. The samples were prepared using a two-step process: in the first step TPS was obtained using a ratio of glycerol/starch 35 wt%/65 wt% which was melt-blended with PBAS and nanofillers in the second step. The compositions of obtained samples are listed in Table 2. PBAS and PBASCl were directly compounded at 120 °C for 10 min with screw speed of 100 rpm.

Specimens for DMTA and XRD were prepared by compression moulding at 5 MPa, 150 °C for 2 min.

Table 1
Mechanical properties of PBAS (PBI 001 datasheet Natureplast).

Properties	Unit	Value
Melting temperature	°C	115
Tensile stress (yield)	MPa	35
Tensile stress (break)	MPa	40
Tensile strain (break)	%	250
Flexural modulus	MPa	650

Table 2
Composition of melt-blended samples.

Sample	TPS (wt%)	PBAS (wt%)	ClNa (wt%)	Cl30B (wt%)
TPS	100.0	–	–	–
TPSCl30B	95.0	–	–	5.0
TPSClNa	95.0	–	5.0	–
TPSPBAS20	80.0	20.0	–	–
TPSPBAS19Cl30B	76.0	19.0	–	5.0
TPSPBAS19ClNa	76.0	19.0	5.0	–
PBAS	–	100.0	–	–
PBASCl30B	–	95	–	5.0

2.2. Analyses

X-ray diffraction-analyses (XRD) were performed on compression moulded specimens using Cu–Kα X-ray source (λ = 1.540562 Å), step-size 0.02° at 2° min^{-1} scanning rate.

Field Emission Scanning Electron Microscope (FE-SEM) examinations were performed with a Zeiss Supra™ 40 (FE-SEM) on surface of fragile fracture obtained after cooling by immersion of specimens in liquid nitrogen. The samples were coated with chromium. Elemental analyses on the surface were made by Energy Dispersive X-ray Spectroscopy or EDS.

Specimens for TEM characterizations were microtomed at −196 °C with an Ultramicrotome Leica UCT, thickness was about 90 nm. The grid was 50 meshes, coated with SPI-Chem™ Pioloform® B Resin. The analyses were performed with a Philips CM 120.

Dynamic-mechanical thermal experiments (DMTA) were performed using a DMA TA Q800 with tension film clamp. Samples 6 mm width × 26 mm height × 1 mm thick were used. The temperature range was from −60 °C to 120 °C, heating rate 3 °C/min, 1 Hz frequency, strain-controlled mode with 15 μm of amplitude, static loading of 125% of dynamic loading and 0.01 N of preload. Experiments were stopped when the sample modules fall below 10 MPa. All the samples were conditioned at 25 °C and 50% RH, in a climate-controlled chamber Binder BFK240. The tests were performed after 1 day conditioning and also after ageing in the same conditions for 15 days.

3. Results and discussion

Fig. 3a shows XRD analyses for TPS and starch. The A-type crystallinity is observed for typical maize starch as evidenced by reflections at 2θ 15.1°, 17.2°, 18.0° and 23.1° (van Soest, Hullemana, de Wita, & Vliegenthar, 1996) which completely disappear in TPS sample. The characteristic peak around 19.9° is due to processing-induced crystallinity of single-helical amylose and observed for extruded and compression molded TPS (van Soest et al., 1996). This peak is present in all the samples containing TPS (Fig. 3a–f). In Fig. 3b, the XRD of pure PBAS is compared with TPSPBAS20, the crystalline structure of PBAS is retained as evidenced by the presence of the peak at 22.7°.

Melt blending of TPS with ClNa (TPSClNa) leads to an increase of interlayer distance (d_{001}) from 1.16 nm to 1.73 nm as calculated by Bragg's law for shift of diffraction peak of ClNa from 7.6° to 5.0° (Fig. 3c). There is no further increase in d_{001} by addition of PBAS (TPSPBAS19ClNa) as shown in Fig. 3d. The presence of this diffraction peak reveals that these materials are mainly intercalated. The same results were reported by Chivrac, Pollet, et al. (2008) and this d_{001} was attributed to the intercalation of glycerol thus few starch chains have been intercalated into the ClNa layers. On blending TPS only with Cl30B (TPSCl30B) there is no change in d_{001} (Fig. 3e) indicating poor miscibility between clay layers glycerol and/or starch. This effect was previously reported (Chiou et al., 2007) and explained as an interaction starch–glycerol higher

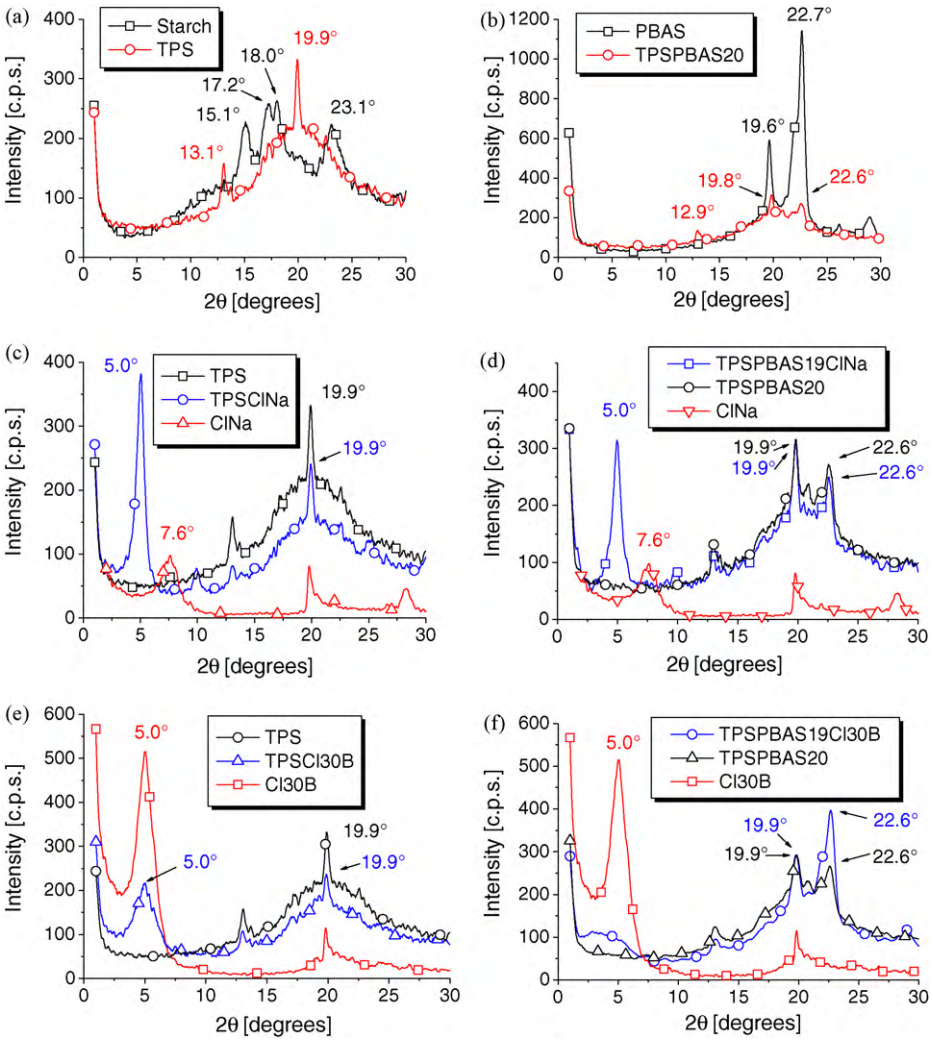

Fig. 3. X-ray analyses of (a) starch and TPS, (b) PBAS and TPSPBAS20, (c) TPS, ClNa and TPSClNa, (d) ClNa, TPSPBAS20 and TPSPBAS19ClNa, (e) TPS, Cl30B and TPSCl30B, (f) Cl30B, TPSPBAS20 and TPSPBAS19Cl30B. (For interpretation of the references to color in this figure legend, the reader is referred to the web version of the article.)

than glycerol–clay preventing the intercalation/exfoliation of the organoclay. In the XRD of the blend containing 19% of PBAS (TPSPBAS19Cl30B) there are no evidence of notable peaks d_{001} except a small and broad diffraction peak is present between 2° and 6° (Fig. 3f) which suggests exfoliation of clay platelets.

PBASCl30B nanocomposite was investigated in order to understand the contribution of PBAS to Cl30B exfoliation. The XRD analyses of PBASCl30B were performed. PBAS chains intercalated into the Cl30B layers as the d_{001} increases from 1.78 nm to 3.26 nm as shown in Fig. 4. This intercalation is promoted by the high affinity of Cl30B surfactant molecules with PBAS because of the close solubility parameters as already demonstrated by Sinha Ray and Bousmina (2005).

FE-SEM was used to investigate the morphology of TPS and TPS blend nanocomposites. FE-SEM analysis (Fig. 4a and b) shows the presence of granules inside TPS with no relevant differences in the chemical composition (Table 3). The heterogeneity observed could be explained by the high glycerol content of the plasticized starch formulation, which is known to induce a phase separation between low and high glycerol content domains (Avérous, 2004; Chivrac, Pollet, & Avérous, 2009; Forssell, Mikkilä, Moates, & Parker, 1997). FE-SEM analyses also show the preserved starch heterogeneous structure in blends with clays and PBAS (Fig. 5). These granules are composed mainly of starch/glycerol. The clays are not present in these domains as demonstrated by semi-quantitative elemental analyses of these regions in the different samples (Table 3). The same nanofiller heterogeneous distributions were obtained by Chivrac, Pollet, et al. (2008) and Chivrac et al. (2010) for TPS-based nanocomposites. In TPSPBAS20 PBAS presence is attested by plastic deformation, the white dots on the fracture surface (Fig. 5g and h).

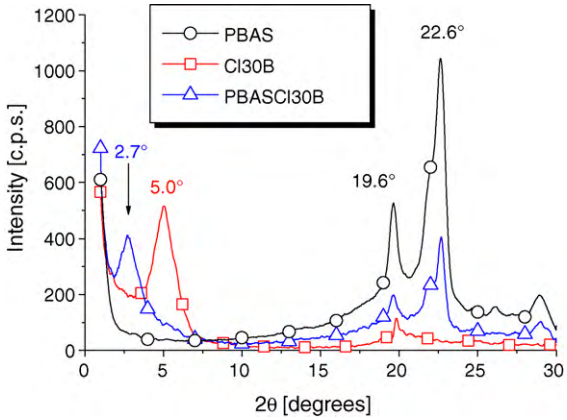

Fig. 4. X-ray analyses of PBAS, Cl30B and PBASCl30B. (For interpretation of the references to color in this figure legend, the reader is referred to the web version of the article.)

Table 3
Energy Dispersive X-ray Spectroscopy elemental analyses of FE-SEM picture in Fig. 4.

	Weight %					
	C	Na	Mg	Al	Si	O
TPS_S1	43					57
TPS_S2	43					57
TPSClNa_S1	42	1				57
TPSClNa_S2	39	1		1	4	55
TPSCl30B_S1	43					57
TPSCl30B_S2	42			1	2	56
TPSCl30B_S3	28			6	16	50
TPSPBAS20_S1	43					57
TPSPBAS20_S2	43					57
TPSPBAS19ClNa_S1	14	3	1	11	30	41
TPSPBAS19ClNa_S2	42	1				57
TPSPBAS19ClNa_S3	40	2		1	2	55
TPSPBAS19Cl30B_S1	42				1	57
TPSPBAS19Cl30B_S2	43					57
TPSPBAS19Cl30B_S3	43					57
TPSPBAS19Cl30B_S4	42			1	2	56

Also in this case the starch heterogeneous structure is preserved and the PBAS is mainly distributed in the continuous phase.

The FE-SEM analyses of nanocomposites containing ClNa confirm the XRD data: there is a good dispersion of the clay with small intercalated particle below 200 nm both for TPSClNa and TPSPBASClNa. However, some micrometric aggregates mainly composed of ClNa are observed in TPSPBASClNa (see S1 Fig. 5i). The presence of carbon (Table 3 TPSPBAS19ClNa_S1) is due to adsorption of glycerol. The presence of a less hydrophilic matrix because of the addition of 19 wt% of PBAS could produce the highly hydrophilic ClNa partial aggregation.

It is interesting to note the presence of sodium also in the starch granules of both ClNa nanocomposites (Table 3). It can be proposed that during the processing the starch or glycerol are partially oxidised in the presence of air during processing, with the formation of carboxylic acid which could exchange protons with the sodium ions present in clay. On the other hand the impurities such as lipids, proteins and phosphate present in the samples could also be the responsible of the exchanged protons.

The FE-SEM analyses show that Cl30B dispersion in the starch-based nanocomposite TPSCl30B (Fig. 5e and f) is similar to that of ClNa in TPSClNa. These results are different from that obtained by

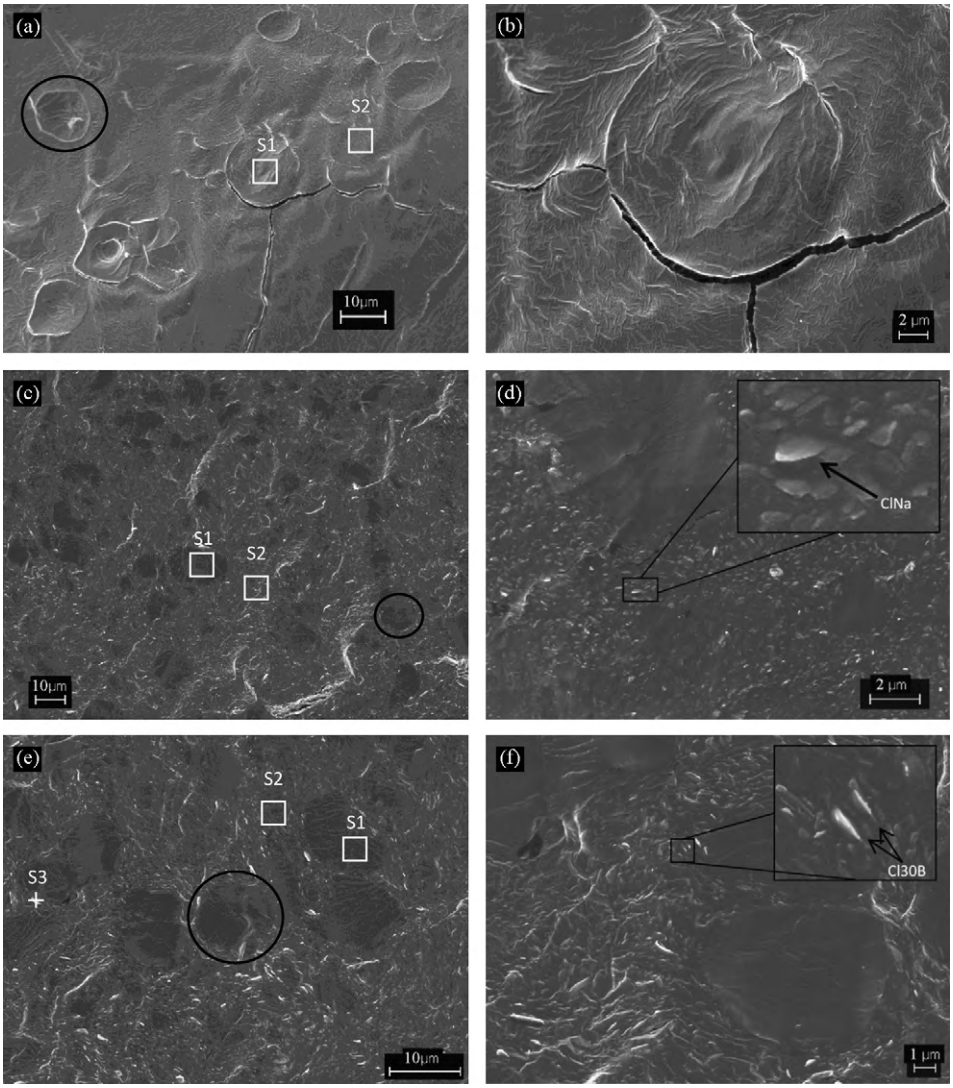

Fig. 5. FE-SEM images of (a) and (b) TPS, (c) and (d) TPSClNa (in the magnification a platelet of ClNa is evidenced), (e) and (f) TPSCl30B (in the magnification a platelet of Cl30B is evidenced), (g) and (h) TPSPBAS20 (PBAS elastic fracture is evidenced), (i) and (j) TPSPBAS19ClNa (in the magnification a platelet of ClNa and PBAS elastic fracture are evidenced), (k) and (l) TPSPBAS19Cl30B elemental analyses of the different marks were reported in Table 2. The "phase separation" is evidenced by black circles.

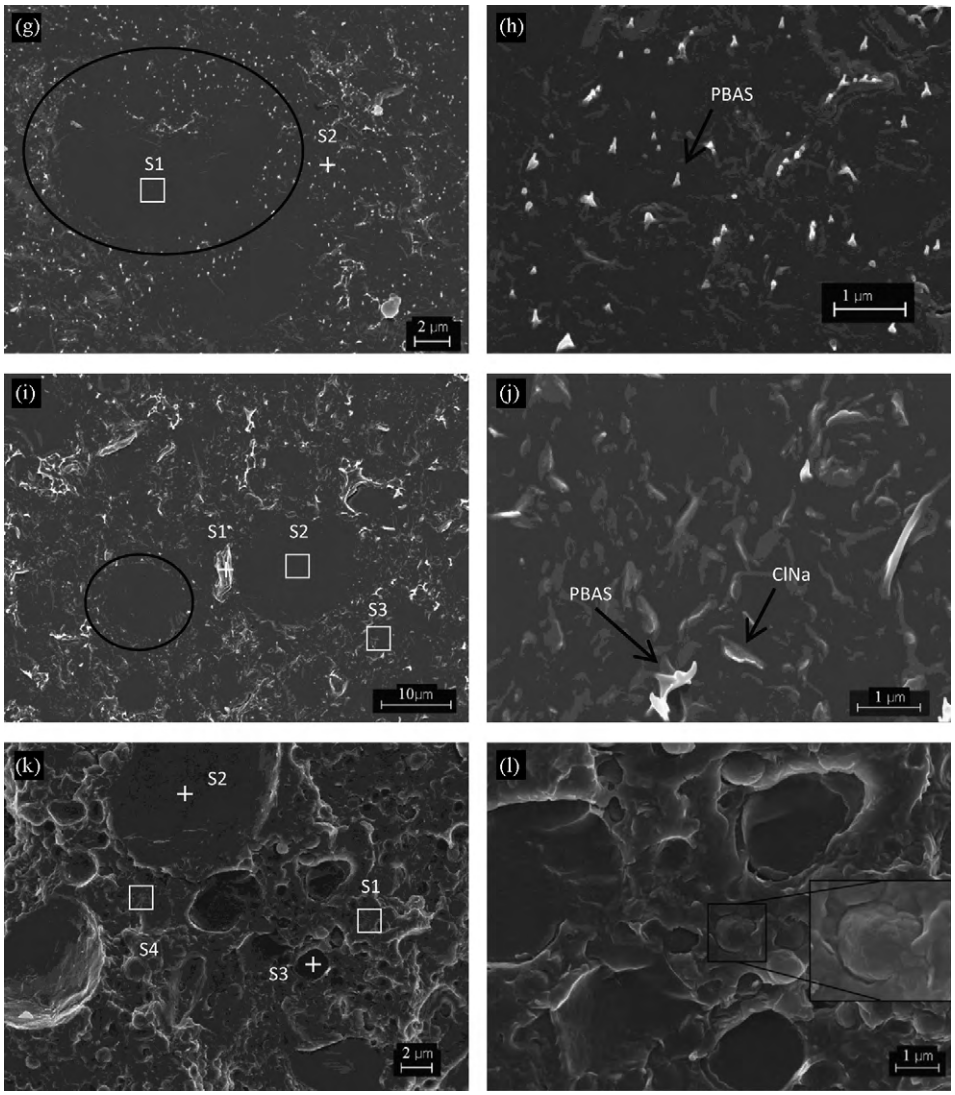

Fig. 5. (*Continued*).

Park et al. (2003), they observed the intercalation and partial exfoliation of Cl30B in a potato starch/water/glycerol in weight ratio of 5/2/3.

As already anticipated from the XRD, the structure of the nanocomposite TPSPBAS19Cl30B is completely different from previous ones (Fig. 5k and l). The structure consists in two different phases, the continuous matrix and the dispersed phase formed by granules with a wide dispersion: from 200 nm up to 10 μm of diameter. From semi-quantitative analyses, the silicon and aluminium is present only in the continuous phase (Table 3) and thus Cl30B is dispersed only in this phase.

The TEM pictures of the continuous phase (Fig. 6) show almost individually dispersed layers attesting the exfoliated morphology for TPSPBAS19Cl30B. It can be proposed that the continuous phase is composed of PBAS/starch/glycerol and Cl30B while the dispersed phase is composed of starch and glycerol. The addition of PBAS could have work as compatibiliser and allowed exfoliation by intercalation of PBAS molecules into Cl30B structure.

The mechanical properties of samples were evaluated using DMTA analysis (Figs. 7 and 8, Table 4). Storage modulus of pure TPS at 25 °C after 1 day is 20 MPa. The storage modulus of TPS nanocomposites (TPSClNa and TPSCl30B) are quite similar, respectively 37 MPa for TPSClNa and 14 MPa for TPSCl30B. Moreover, it is not possible to measure the modulus at high temperature (85 °C) for these samples. This low reinforcement effect of both nanoparticles can be explained by the absence of starch intercalation in both nanocomposites thus the nanoparticles act as a traditional filler.

The addition of PBAS to TPS results in a small increase of storage modulus at room temperature (29 MPa). The module at 85 °C (12 MPa) was less than what expected from quantitative addition of the TPS and PBAS modules.

The nanocomposite TPSPBAS19ClNa shows an increase in the storage modulus at 25 °C (46 MPa) respect to TPSPBAS20. This limited increase is probably linked to the partial subtraction of glycerol from ClNa.

An effective reinforcement effect is achieved in TPSPBASCl30B. The exfoliated nanocomposite has the highest modulus which is about 10 times higher than the same nanocomposite with ClNa at both temperatures (25 °C and 85 °C) and obviously even more respect to the pure TPS and the TPSPBAS. The storage modulus at 25 °C is 470 MPa which is quite similar to pure PBAS (600 MPa) and it remains high (190 MPa) even at high temperature (85 °C) equivalent to the 65% of pure PBAS modulus at the same temperature. The presence of PBAS in the TPSPBAS19Cl30B continuous phase is confirmed by the shut in modulus near to PBAS melting temperature (≈115 °C) (Fig. 6a).

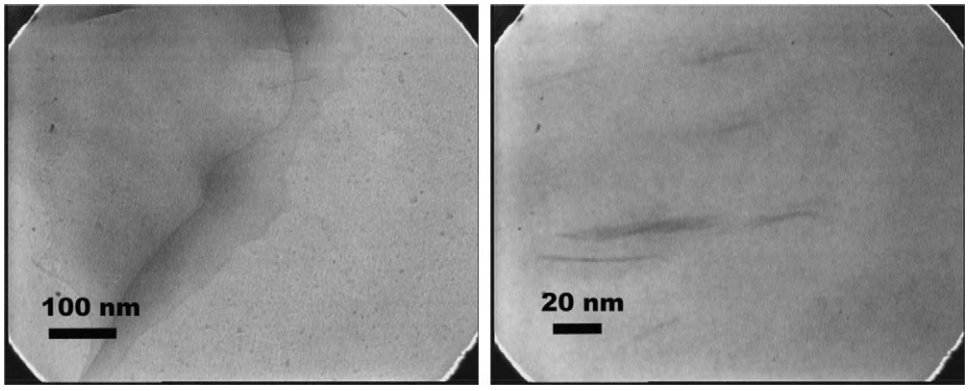

Fig. 6. TEM analyses of TPSPBAS19Cl30B.

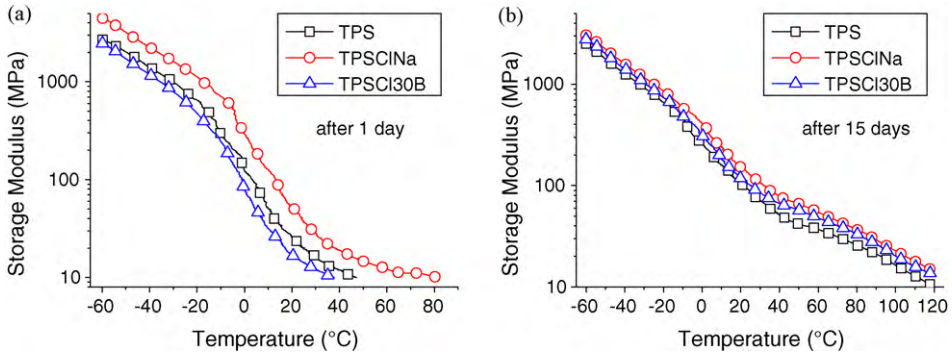

Fig. 7. Storage modulus of TPS, TPSClNa and TPSCl30B nanocomposites after 1 day (a) and after 15 days (b). (For interpretation of the references to color in this figure legend, the reader is referred to the web version of the article.)

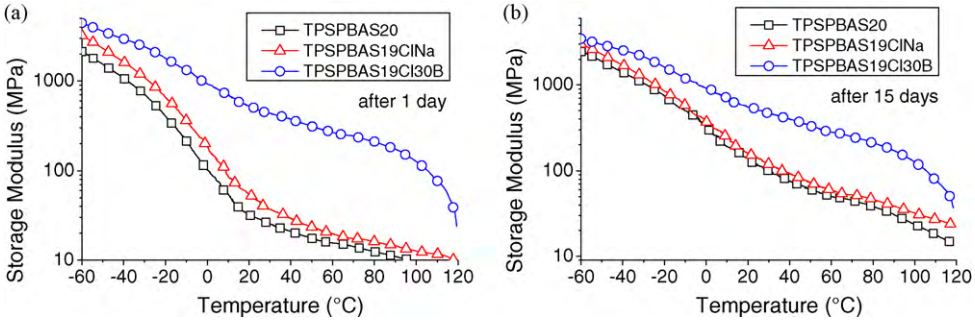

Fig. 8. Storage modulus of TPSPBAS, TPSPBAS19ClNa and TPSPBAS19Cl30B nanocomposites after 1 day (a) and after 15 days (b). (For interpretation of the references to color in this figure legend, the reader is referred to the web version of the article.)

Different authors (Avérous, 2004; Smits, Hulleman, van Soest, Feil, & Vliegenthart, 1999; van Soest & Knooren, 1997) have shown that after processing, TPS undergo aging with a strong evolution of mechanical properties. TPS presents two kinds of aging behaviour depending on glass transition temperature and conditioning temperature. Conditioning TPS in the sub-T_g domain, TPS shows a physical aging versus time, with a material densification (Lourdin, Colonna, Brownsey, Noel, & Ring, 2002; Smits et al., 1999). In the case of storing temperature above T_g, TPS shows retrogradation phenomena with the evolution of the crystallinity

Table 4
Storage modulus of melt-blended samples after 1 day (d1) and after 15 days (d15).

Sample	Modulus@ 25 °C d1 (MPa)	Modulus@ 85 °C d1 (MPa)	Modulus@ 25 °C d15 (MPa)	Modulus@ 85 °C d15 (MPa)
TPS	20	<10[a]	87	23
PBAS	600	290	600	290
TPSClNa	37	<10[a]	126	33
TPSCl30B	14	<10[a]	100	30
TPSPBAS20	29	12	115	35
TPSPBAS19ClNa	46	15	139	42
TPSPBAS19Cl30B	470	190	505	191

[a] Test stopped because module falls below 10 MPa.

and rearrangements of plasticizer molecules into the material (van Soest & Knooren, 1997). The starch in TPS tends to crystallise and to lost part of the plasticizer thus there is an increase of the tensile modulus, which increase during several weeks, and a reduction of elongation at break. The starch becomes thus more brittle. The retrogradation kinetic depends on the macromolecules mobility, on the plasticizer type and content (Smits et al., 1999). The samples tested were stored above glass transition temperature in a conditioned chamber (25 °C, 50% RH) for 15 days. The storage modulus (Fig. 5b) of TPS blends and nanocomposites are increased (from about 3 to 7 times) in accord with formation of starch crystalline structure. The storage modulus of the TPSPBAS19Cl30B is almost constant even after 15 days confirming the importance of PBAS in the continuous phase and that the presence of exfoliated clay does not allow (or slows) the retrogradation of the material, as already proved for others TPS clay nanocomposites (Magalhães & Andrade, 2009).

4. Conclusions

Melt blending of TPS with ClNa and Cl30B does not lead to exfoliation or intercalation of starch chains into the clay layers thus there are no significant mechanical reinforcement effects. The same results are obtained on blending TPS with ClNa and PBAS because of the absence of interaction between highly hydrophilic ClNa and hydrophobic PBAS. On blending TPS with Cl30B and PBAS an exfoliated nanocomposite is formed. The exfoliation is promoted by the high affinity between Cl30B and PBAS. PBAS promote exfoliation by intercalation into Cl30B structure. The resulting nanocomposite shows a multiphase structure. A segregated particle structure starch/glycerol is formed while the continuous phase is characterized by high concentration in PBAS and organoclay. The final blend, thanks to the higher modulus of PBAS and the contemporaneous presence of exfoliated organoclay, is characterized by a considerable increase of the modulus with respect to TPS alone.

Acknowledgments

The authors thank Prof. Giovanni Camino (Politecnico di Torino sede di Alessandria) for the useful discussions and comments. We would like to express our thanks to Dr. Domenico Mombello (Politecnico di Torino DISMIC) for the FE-SEM analyses.

References

Amass, W., Amass, A., & Tighe, B. (1999). A review of biodegradable polymers: Uses, current developments in the synthesis and characterization of biodegradable polyesters, blends of biodegradable polymers and recent advances in biodegradation studies. *Polymer International*, *97*(2), 89–144.

Avérous, L. (2004). Biodegradable multiphase systems based on plasticized starch: A review. *Polymer Reviews*, *44*(3), 231–274.

Avérous, L., & Fringant, C. (2001). Association between plasticized starch and polyesters: Processing and performances of injected biodegradable systems. *Polymer Engineering and Science*, *41*(5), 727–734.

Avérous, L., Moro, L., Dole, P., & Fringant, C. (2000). Properties of thermoplastics blends: Starch–polycaprolactone. *Polymer*, *41*(11), 4157–4167.

Bastioli, C. (1998). Biodegradable materials—Present situation and future perspectives. *Macromolecular Symposia*, *135*, 193–204.

Bastioli, C., Cerruti, A., Guanella, I., Romano, G. C., & Tosin, M. (1995). Physical state and biodegradation behavior of starch–polycaprolactone systems. *Journal of Polymers and the Environment*, *3*(2), 81–95.

Belgacem, M. N., & Gandini, A. (2008). The state of the art. In *Monomers polymers and composites from renewable resources*. Amsterdam: Elsevier., pp. 1–16.

Bhattacharya, M. (1998). Stress relaxation of starch/synthetic polymer blends. *Journal of Materials Science*, *33*(16), 4331–4339.

Chiou, B. S., Wood, D., Yee, E., Imam, S. H., Glenn, G. M., & Orts, W. J. (2007). Extruded starch–nanoclay nanocomposites: Effects of glycerol and nanoclay concentration. *Polymer Engineering and Science*, *47*(11), 1898–1904.

Chivrac, F., Gueguen, O., Pollet, E., Ahzi, S., Makradi, A., Avérous, L., et al. (2008). Micromechanical modeling and characterization of the effective properties in starch based nano-biocomposites. *Acta Biomaterialia*, *4*(6), 1707–1714.

Chivrac, F., Pollet, E., & Avérous, L. (2009a). Shear induced clay organo-modification: Application to plasticized starch nano-biocomposites. *Polymers for Advanced Technologies*, doi:10.1002/pat.1468

Chivrac, F., Pollet, E., & Avérous, L. (2009b). Progress in nano-biocomposites based on polysaccharides and nanoclays. *Materials Science and Engineering: R: Reports*, *67*(1), 1–17.

Chivrac, F., Pollet, E., Schmutz, M., & Avérou, L. (2008). New approach to elaborate exfoliated starch-based nanobiocomposites. *Biomacromolecules*, *9*(3), 896–900.

Chivrac, F., Pollet, E., Schmutz, M., & Avérous, L. (2010). Starch nano-biocomposites based on needle-like sepiolite clays. *Carbohydrate Polymers*, *80*(1), 145–153.

Cyras, V. P., Manfredi, L. B., Ton-That, M., & Vázquez, A. (2008). Physical and mechanical properties of thermoplastic starch/montmorillonite nanocomposite films. *Carbohydrate Polymers*, *73*(1), 55–63.

Dean, K., Yu, L., & Wu, D. (2007). Preparation and characterization of melt-extruded thermoplastic starch/clay nanocomposites. *Composites Science and Technology*, *67*(3–4), 413–421.

Forssell, P. M., Mikkilä, J. M., Moates, G. K., & Parker, R. (1997). Phase and glass transition behaviour of concentrated barley starch–glycerol–water mixtures: A model for thermoplastic starch. *Carbohydrate Polymers*, *34*(3), 275–282.

Fringant, C., Desbrieres, J., & Rinaudo, M. (1996). Physical properties of acetylated starch-based materials: Relation with their molecular characteristics. *Polymer*, *37*(13), 2663–2673.

Koenig, M. F., & Huang, S. J. (1995). Biodegradable blends and composites of polycaprolactone and starch derivatives. *Polymer*, *36*(9), 1877–1882.

Lourdin, D., Colonna, P., Brownsey, G. J., Noel, T. R., & Ring, S. G. (2002). Structural relaxation and physical aging of starchy materials. *Carbohydrate Research*, *337*(9), 827–833.

Ma, X., Yu, J., & Wang, N. (2007). Production of thermoplastic starch/MMT-sorbitol nanocomposites by dual-melt extrusion processing. *Macromolecular Materials and Engineering*, *292*(6), 723–728.

Magalhães, N. F., & Andrade, C. T. (2009). Thermoplastic corn starch/clay hybrids: Effect of clay type and content on physical properties. *Carbohydrate Polymers*, *75*(4), 712–718.

Martin, O., & Avérous, L. (2001). Poly (lactic acid): Plasticization and properties of biodegradable multiphase systems. *Polymer*, *42*(14), 6209–6219.

Matzinos, P., Tserki, V., Kontoyiannis, A., & Pan, C. (2001). Processing and characterization of starch/polycaprolactone products. *Polymer Degradation and Stability*, *77*(1), 17–24.

Mullen, J. W., & Pacsu, E. (1942). Starch studies: Preparation and properties of starch trimesters. *Journal of Industrial & Engineering Chemistry*, *34*(10), 1209–1217.

Mullen, J. W., & Pacsu, E. (1943). Starch studies. Possible industrial utilization of starch esters. *Journal of Industrial & Engineering Chemistry*, *35*(3), 381–384.

Myllymäki, O., Myllärinen, P., Forssell, P., Suortti, T., Lähteenkorva, K., & Ahvenainen, R. (1998). Mechanical and permeability properties of biodegradable extruded starch/polycaprolactone films. *Packaging Technology and Science*, *11*(6), 265–274.

Pandey, J. K., & Singh, R. P. (2005). Green nanocomposites from renewable resources: Effect of plasticizer on the structure and material properties of clay-filled starch. *Starch - Stärke*, *57*(1), 8–15.

Park, H., Lee, W., Park, C., Cho, W., & Ha, C. (2003). Environmentally friendly polymer hybrids. Part I. Mechanical, thermal, and barrier properties of thermoplastic starch/clay nanocomposites. *Journal of Materials Science*, *38*(5), 909–915.

Park, H., Li, X., Jin, C., Park, C., Cho, W., & Ha, C. (2002). Preparation and properties of biodegradable thermoplastic starch/clay hybrids. *Macromolecular Materials and Engineering*, *287*(8), 553–558.

Shogren, R. (1997). Water vapor permeability of biodegradable polymers. *Journal of Polymers and the Environment*, *5*(2), 1566–2543.

Sinha Ray, S., & Bousmina, M. (2005). Poly (butylene sucinate-co-adipate)/montmorillonite nanocomposites: Effect of organic modifier miscibility on structure, properties, and viscoelasticity. *Polymer*, *46*(26), 12430–12439.

Smits, A. L. M., Hulleman, S. H. D., van Soest, J. J. G., Feil, H., & Vliegenthart, J. F. G. (1999). The influence of polyols on the molecular organization in starch-based plastics. *Polymers for Advanced Technologies*, *10*(10), 570–573.

van Soest, J. J. G., Hullemana, S. H. D., de Wita, D., & Vliegenthar, J. F. G. (1996). Crystallinity in starch bioplastics. *Industrial Crops and Products*, *5*(2), 11–22.

van Soest, J. J. G., & Knooren, N. (1997). Influence of glycerol and water content on the structure and properties of extruded starch plastic sheets during aging. *Journal of Applied Polymer Science*, *64*(7), 1411–1422.

Vikman, M., Hulleman, S. H. D., Van Der Zee, M., Myllärinen, P., & Feil, H. (1999). Morphology and enzymatic degradation of thermoplastic starch–polycaprolactone blends. *Journal of Applied Polymer Science*, *74*(11), 2594–2604.

Wiedmann, W., & Strobel, E. (1991). Compounding of thermoplastic starch with twin-screw extruders. *Starch - Stärke*, *43*(4), 138–145.